Outage Probability of Multi-Carrier NOMA Systems under Joint I/Q Imbalance

(Invited Paper)

Bassant Selim*, Sami Muhaidat*, Paschalis C. Sofotasios*,‡, Bayan S. Sharif*, Thanos Stouraitis*, George K. Karagiannidis§, and Naofal Al-Dhahir¶

*Department of Electrical and Computer Engineering, Khalifa University of Science and Technology, 127788, Abu Dhabi, United Arab Emirates
(e-mail: {bassant.selim; sami.muhaidat; paschalis.sofotasios; bayan.sharif; thanos.stouraitis}@ku.ac.ae)
‡Department of Electronics and Communications Engineering, Tampere University of Technology, FI-33101, Tampere, Finland, (e-mail: paschalis.sofotasios@tut.fi)
§Department of Electrical and Computer Engineering, Aristotle University of Thessaloniki, GR-51124, Thessaloniki, Greece, (e-mail: geokarag@auth.gr)
¶Department of Electrical and Computer Engineering, University of Texas at Dallas, TX 75080, Dallas, USA, (e-mail: aldhahir@utdallas.edu)

***Abstract*—Non-orthogonal multiple access (NOMA) has been recently proposed as a viable technology that can potentially improve the spectral efficiency of fifth generation (5G) wireless networks and beyond. However, in practical communication scenarios, transceiver architectures inevitably suffer from radio-frequency (RF) front-end related impairments that can lead to degradation of the overall system performance, with in-phase/quadrature-phase imbalance (IQI) constituting a major impairment in direct-conversion transceivers. In the present work, we quantify the effects of joint transmitter/receiver IQI on the performance of NOMA based multi-carrier (MC) systems under multipath fading conditions. Furthermore, we derive the asymptotic diversity order of the considered MC NOMA set up. Capitalizing on these results, we demonstrate that the effects of IQI differ considerably among NOMA users and depend on the underlying system parameters. For example, it is shown that the first sorted user appears more robust to IQI, which indicates that higher order users are more sensitive to the considered non-negligible impairment.**

I. Introduction

The emergence of the Internet of Things (IoT) together with the ever-increasing demands of mobile Internet impose high spectral efficiency and massive connectivity requirements on fifth generation (5G) wireless networks and beyond. Furthermore, future communication systems are expected to support heterogeneous devices with various service types, essential high throughput and low latency requirements. Based on this, non-orthogonal multiple access (NOMA) was recently introduced as an effective approach that is capable of overcoming these challenges, rendering it a promising candidate for 5G systems and beyond. The distinct characteristic of NOMA is that it can be realized by allowing multiple users to share the same frequency bands and time slots through power-domain or code-domain multiplexing, while successive interference cancellation (SIC) is utilized to enable elimination of the resulting multi-user interference.

The key concept underlying NOMA is to make use of non-orthogonal resources, such as power or code-domain for multiple access (MA), instead of the time or frequency domain, as in orthogonal multiple access (OMA) schemes. Also, contrary to OMA schemes, NOMA does not allocate orthogonal resources to the different users and it instead performs SIC. Hence, NOMA can provide better spectral efficiency, higher cell-edge throughput and relaxed channel feedback as only the received signal strength is practically required. In addition, it is capable of providing low transmission latency since scheduling requests from users to the base station are not necessary [1]. Moreover, the number of supported users in OMA is strictly restricted to the amount of available resources, whereas the non-orthogonal resource allocation in NOMA can potentially lead to a significant increase of the number of connected devices in the network [2], [3].

A critical component of the massive number of interconnected devices is the radio frequency (RF) transceiver, which facilitates communication between the individual devices and/or their respective base stations. However, the continuously increasing demands in applications of RF transceivers has led to harsh design targets including increased performance and efficiency, low cost, low power dissipation, and small form factor. In this context, direct-conversion transceivers represent an effective RF front-end solution, as they demand neither external intermediate frequency filters nor image rejection filters. Hence, these transceiver architectures can be integrated on chip fairly easily while their cost is rather low. However, in practical communication scenarios, these monolithic architectures suffer from inevitable RF front-

978-1-5386-4609-0/18/$31.00 ©2018 IEEE

end related imperfections due to components mismatch and manufacturing nonidealities, which limit the overall system performance. A critical example of these impairments is the in-phase (I)/quadrature-phase (Q) imbalance (IQI), which refers to the amplitude and phase mismatch between the I and Q branches of the transceiver, leading to imperfect image rejection, and ultimately resulting to performance degradation of the overall communication system [4], [5]. In ideal scenarios, the I and Q branches of a mixer have equal amplitude and a phase shift of $90°$, providing an infinite attenuation of the image band; however, in practice, direct-conversion transceivers are sensitive to certain analog front-end related impairments that introduce errors in the phase shift as well as mismatches between the amplitudes of the I and Q branches which corrupt the down-converted signal constellation, thereby increasing the corresponding error rate [4].

In spite of the impact of RF front-end impairments on the system performance, their detrimental effect is often neglected. Therefore, it is necessary to investigate this topic, which despite its paramount importance for the actual realization of NOMA systems, it has not yet, to the best of the authors' knowledge, been addressed in the open technical literature [6]. Motivated by this, the present investigation is devoted to the quantification and analysis of the effects of IQI on multi-carrier (MC) NOMA based systems over multipath fading channels. To this end, we quantify the effects of IQI on the considered NOMA based system by means of the corresponding outage probability (OP) analysis subject to IQI effects at both the transmitter (TX) and receiver (RX). This analysis provides meaningful insights on the behavior and performance of the considered set up, which are expected to be useful in the design and deployment of future NOMA based systems.

II. System Model

It is recalled that the basic idea behind NOMA is to allow a certain level of interference from adjacent users by allocating non-orthogonal resources to the different users in the network. In the present investigation, we consider the case of downlink NOMA where all users are served by a BS at the same time and frequency, but with different power levels. It is worth mentioning that power domain multiplexing NOMA can be efficiently realized by applying superposition coding at the TX and SIC at the RX. Hence, in order to serve several users simultaneously, the BS divides its transmission power between all users, while at the receiver end, multi-user detection is performed using SIC [2].

One of the key challenges in NOMA is how to allocate the power amongst the involved users. A common and fairly simple power allocation strategy is the fixed power allocation, where the power ratios are fixed and ordered according to the users' channel gains. In this scenario, we assume that more power is allocated to users with poorer channel conditions. In this context, we assume a single-cell NOMA downlink system consisting of a BS and M users, depicted in Fig. 1, with transceivers equipped with a single antenna. Based on this, we let h_i represent the small scale fading coefficient between the i^{th} user and the BS which follows a Rayleigh distribution. Therefore, for $|h_1|^2 \leq |h_2|^2 \leq ... \leq |h_M|^2$, and assuming an ideal RF front end, the baseband equivalent transmitted signal is given by [7]

$$x = \sum_{i=1}^{M} \sqrt{P_i} s_i \tag{1}$$

where $P_i = a_i E_t$ and s_i are the power and information symbol of the i^{th} sorted user, respectively, E_t is the transmit power of the BS, $\sum_{i=1}^{M} a_i = 1$ and $a_1 > a_2 > ... > a_M$. At the receiver RF front end, the received RF signal undergoes the necessary processing stages including filtering, amplification, analog I/Q demodulation (down-conversion) to baseband and sampling. Hence, assuming an ideal RF front end, the baseband equivalent received signal at the j^{th} sorted user is given by

$$r_j = h_j \sum_{i=1}^{M} \sqrt{P_i} s_i + n_j \tag{2}$$

where the subscript j refers to the j^{th} sorted user while h and n denote the channel coefficient and circularly symmetric complex additive white Gaussian noise (AWGN) signal, respectively. The j^{th} sorted user then performs SIC in order to cancel the resulted interference for all users i, where $i < j$, whereas the signals intended for all other users with $i > j$ are treated as noise. Hence, assuming perfect channel state information (CSI) and perfect cancellation, the instantaneous SINR per symbol of the m^{th} user's message at the j^{th} sorted user, $m < j$, is given by [8]

$$\gamma_{j \to m} = \frac{a_m}{\sum\limits_{i=m+1}^{M} a_i + \frac{1}{\rho_j}} \tag{3}$$

where ρ_j is the j^{th} user's instantaneous signal-to-noise ratio (SNR) given by

$$\rho_j = \frac{E_t}{N_0} |h_j|^2 \tag{4}$$

where N_0 is the single-sided AWGN power spectral density.

Although NOMA has exhibited capacity improvement and reduced latency, it suffers from several drawbacks, particularly, in small cells, where users could possibly experience similar channel conditions. In this respect, NOMA is envisioned to co-exist with other OMA schemes, such as orthogonal frequency division multiple access (OFDMA), which will result in a significantly better overall performance and, potentially, fulfill the diverse requirements of different wireless services and applications [9]. It is recalled that MC systems are based on the division of the available signal bandwidth among K subcarriers, which has been shown to have several advantages, such as enhanced robustness against multipath fading. Based on this, Long-Term Evolution (LTE) employs orthogonal frequency division multiplexing (OFDM), which is a MC modulation with orthogonal subcarriers, in the downlink transmission.

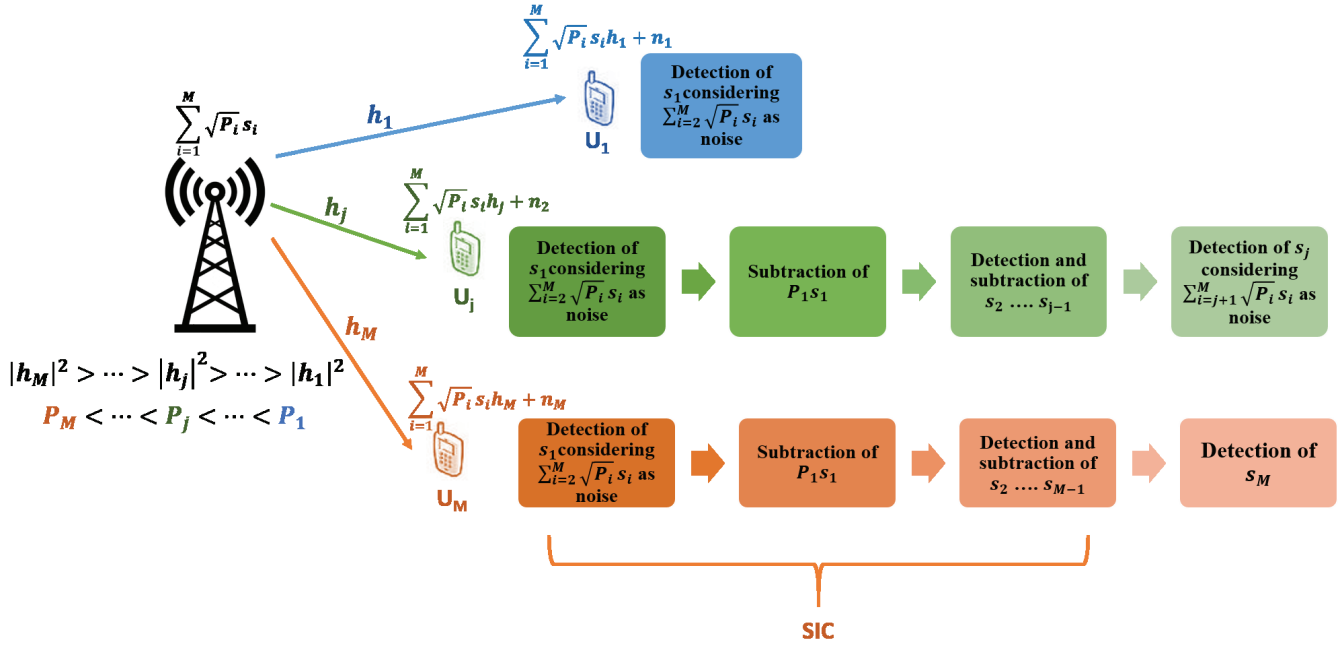

Fig. 1: Typical M user NOMA communication scenario.

In what follows, we derive the SINR CDF and the OP of MC NOMA systems in the presence of IQI assuming that the RF subcarriers are down converted to the baseband by wideband direct conversion. We also denote the set of subcarriers as

$$S = \left\{-\frac{K}{2}, ..., -1, 1, ..., \frac{K}{2}\right\} \tag{5}$$

and assume that there is an information signal present at the image subcarrier and that the channel responses at the k^{th} subcarrier and its image are uncorrelated.

It is noted here that the exact modeling and simulation of the RF front-end is typically complex and time consuming. Thus, applying baseband equivalent impairment models, instead of modeling the actual RF front-end, represents a pragmatic approach to the analysis of RF related impairments as this modeling relates the baseband representation to the bandpass signal with the RF impairments [10]. Based on this, we assume that the RF subcarriers in the present analysis are up/down converted to the baseband by direct conversion architectures and consider frequency independent IQI caused by the gain and phase mismatches of the I and Q mixers. Thus, the time-domain baseband representation of the IQI impaired signal is given by [11]

$$g_{\text{IQI}} = \mu_{t/r} g_{\text{id}} + \nu_{t/r} g_{\text{id}}^{*} \tag{6}$$

where $(\cdot)^*$ denotes conjugation, g_{id} is the baseband IQI-free signal, g_{id}^{*} is due to IQI and the subscripts t/r denote the up/down-conversion process at the TX/RX, respectively. Furthermore, the IQI coefficients $\mu_{t/r}$ and $\nu_{t/r}$ are expressed as [10]

$$\mu_t = \frac{1}{2}\left(1 + \epsilon_t \exp\left(j\phi_t\right)\right), \tag{7}$$

$$\nu_t = \frac{1}{2}\left(1 - \epsilon_t \exp\left(-j\phi_t\right)\right), \tag{8}$$

$$\mu_r = \frac{1}{2}\left(1 + \epsilon_r \exp\left(-j\phi_r\right)\right) \tag{9}$$

and

$$\nu_r = \frac{1}{2}\left(1 - \epsilon_r \exp\left(j\phi_r\right)\right) \tag{10}$$

respectively, where $j = \sqrt{-1}$, whilst $\epsilon_{t/r}$ and $\phi_{t/r}$ are the TX/RX amplitude and phase mismatch levels, respectively. It is noted that for ideal RF front-ends, $\phi_{t/r} = 0°$ and $\epsilon_{t/r} = 1$, which implies that $\mu_{t/r} = 1$ and $\nu_{t/r} = 0$. Moreover, the TX/RX image rejection ratio (IRR) is given by

$$\text{IRR}_{t/r} = \frac{\left|\mu_{t/r}\right|^2}{\left|\nu_{t/r}\right|^2} \tag{11}$$

where $|\cdot|$ denotes absolute value operation. It is noted that in single-carrier (SC) systems, IQI causes distortion to the signal by its own complex conjugate, while in MC systems IQI causes distortion to the transmitted signal at subcarrier k by its image signal at subcarrier $-k$.

To this effect and considering MC NOMA communication scenarios where both the TX and RX suffer from IQI, the j^{th} user's receiver, the baseband equivalent received signal is represented as follows:

$$
\begin{aligned}
r_{j_{\text{IQI}}} = &\left(\xi_{11_j} h_j(k) + \xi_{22_j} h_j^*(-k)\right) \sum_{i=1}^{K} \sqrt{P_i} s_i(k) \\
&+ \left(\xi_{12_j} h_j(k) + \xi_{21_j} h_j^*(-k)\right) \sum_{i=1}^{K} \sqrt{P_i} s_i^*(-k) \\
&+ \mu_{r_j} n_j(k) + \nu_{r_j} n_j^*(-k).
\end{aligned} \tag{12}
$$

Hence, by also assuming perfect CSI and interference cancellation following the SIC, we obtain

$$
\begin{aligned}
r_{j_{\text{IQI}}} = &\left(\left(\xi_{11_j} - 1\right) h_j(k) + \xi_{22_j} h_j^*(-k)\right) \sum_{i=1}^{j-1} \sqrt{P_i} s_i(k) \\
&+ \left(\xi_{11_j} h_j(k) + \xi_{22_j} h_j^*(-k)\right) \sum_{i=j}^{M} \sqrt{P_i} s_i(k) \\
&+ \left(\xi_{12_j} h_j(k) + \xi_{21_j} h_j^*(-k)\right) \sum_{i=1}^{M} \sqrt{P_i} s_i^*(-k) \\
&+ \mu_{r_j} n_j(k) + \nu_{r_j} n_j^*(-k).
\end{aligned} \tag{13}
$$

Notably, since $\mathbb{E}\left[h^2\right] = 0$ and assuming $\mathbb{E}[s_i] = 0$, $\mathbb{E}[s_i s_k] = 0$, at the k^{th} subcarrier, the instantaneous SINR per symbol of the m^{th} user's message at the j^{th} user's receiver is approximated as follows:

$$
\gamma_{j \to m}(k) \approx \frac{\left(|\xi_{11_j}|^2 \rho_j(k) + |\xi_{22_j}|^2 \rho_j(-k)\right) a_m}{\rho_j(k) \mathcal{A}_1 + \mathcal{A}_2} \tag{14}
$$

where $\mathcal{A}_1$ and $\mathcal{A}_2$ are given by

$$
\mathcal{A}_1 = |\xi_{11_j} - 1|^2 \sum_{i=1}^{m-1} a_i + |\xi_{12_j}|^2 + |\xi_{11_j}|^2 \sum_{i=m+1}^{M} a_i \tag{15}
$$

and

$$
\mathcal{A}_2 = \rho_j(-k) \left(|\xi_{22_j}|^2 (1 - a_m) + |\xi_{21_j}|^2\right) + \Xi_{r_j} \tag{16}
$$

respectively, while

$$
\Xi_{r_j} = |\mu_{r_j}|^2 + |\nu_{r_j}|^2. \tag{17}
$$

III. OP of NOMA with IQI

It is recalled that the OP accounts for the probability that the symbol error rate is greater than a certain quality of service requirement and it can be computed as the probability that the SNR or SINR falls below a corresponding threshold, which depends on the detection technique as well as on the modulation order [12].

Proposition 1. *Assuming downlink MC NOMA systems with joint TX/RX IQI, the OP of the j^{th} sorted user is given by*

$$
P_{\text{out},j} = \underbrace{\sum_{l=j}^{M} \sum_{p=0}^{l} \binom{M}{l} \binom{l}{p} \frac{(-1)^p \exp\left(-\frac{\phi_m \Xi_{r_j} (M-l+p) \psi_m}{\overline{\gamma}}\right)}{1 + \psi_m (M - l + p) \mathcal{A}_3}}_{\mathcal{I}_1} \tag{18}
$$

where

$$
\mathcal{A}_3 = \phi_m \left(|\xi_{22_j}|^2 (1 - a_m) + |\xi_{21_j}|^2\right) - |\xi_{22_j}|^2 a_m. \tag{19}
$$

Furthermore, ψ_m is defined as

$$
\psi_m = \max_{1 \le m \le j} \frac{1}{|\xi_{11_j}|^2 a_m - \phi_m \mathcal{A}_4} \tag{20}
$$

where

$$
\mathcal{A}_4 = |\xi_{11_j} - 1|^2 \sum_{i=1}^{m-1} a_i + |\xi_{11_j}|^2 \sum_{i=m+1}^{M} a_i + |\xi_{12_j}|^2 \tag{21}
$$

and

$$
\phi_m = 2^{R_m} - 1 \tag{22}
$$

with R_m denoting the targeted data rate of the m^{th} user. Moreover, equation (18) is valid for

$$
0 \le \phi_m < \frac{|\xi_{11_j}|^2 a_m}{|\xi_{11_j} - 1|^2 \sum_{i=1}^{m-1} a_i + |\xi_{11_j}|^2 \sum_{i=m+1}^{M} a_i + |\xi_{12_j}|^2} \tag{23}
$$

since if the above condition is not satisfied, the OP becomes unity.

Proof. The proof is provided in Appendix A. □

Capitalizing on Proposition 1, the asymptotic diversity order of MC NOMA under IQI is evaluated as [13]

$$
d_a = \lim_{\overline{\gamma} \to \infty} \frac{-\log P_{\text{out}}}{\log \overline{\gamma}}. \tag{24}
$$

To this effect and recalling the asymptotic representation of the exponential function for small argument values, namely

$$
\exp(-x) \underset{x \to 0}{\approx} 1 - x \tag{25}
$$

as well as substituting (18) in (24), it follows that

$$
d_a = \lim_{\overline{\gamma} \to \infty} \frac{-\log(\mathcal{I}_1)}{\log \overline{\gamma}} = 0 \tag{26}
$$

where $\mathcal{I}_1$ is given in (18). Importantly, this reveals that MC NOMA systems with joint TX/RX IQI asymptotically reach an error floor, regardless of the level of IQI considered. This error floor is obtained by setting $\overline{\gamma} = \infty$ in equation (18), yielding

$$P_{\text{out},j}^{\infty} = \sum_{l=j}^{M} \sum_{p=0}^{l} \binom{M}{l} \binom{l}{p} \frac{(-1)^p}{1 + \psi_m \left(M - l + p\right) \mathcal{A}_3}. \quad (27)$$

It is noted here that the above analysis is based on the consideration of an ideal system where the users have perfect knowledge of the corresponding CSI. However, this is not usually the case in realistic practical communication scenarios; as a consequence, the performance of NOMA based communication systems is expected to further degrade under this condition. Hence, the present analysis provides a lower bound on the actual OP performance of NOMA communication systems[1].

IV. Numerical and Simulation Results

Considering the aforementioned NOMA approach, this section investigates the effect of IQI on the performance of NOMA based communication systems. To this end and assuming Rayleigh fading conditions, extensive Monte Carlo simulations have been executed in order to investigate the OP performance of NOMA under IQI effects. It is noted that, unless otherwise stated, the number of users considered is $M = 2$ and that the power allocation coefficients are $a_1 = 4/5$ and $a_2 = 1/5$ for $M = 2$, and $a_1 = 1/2$, $a_2 = 1/3$ and $a_3 = 1/6$, for $M = 3$ [8]. Moreover, for a fair comparison, we assume that the transmit power level is always fixed. This implies that the transmitted signal is normalized by

$$\left(|\mu_t|^2 + |\nu_t|^2\right)\left(|\mu_r|^2 + |\nu_r|^2\right).$$

To this end, Figs. $2-4$ present the OP of MC NOMA based systems in the presence of IQI. It is noted that the numerical results are shown with solid lines, whereas markers are used to illustrate the respective computer simulation results. It is observed that the proposed approximation accurately characterizes the OP of the system.

Fig. 2 depicts the OP of MC NOMA systems as a function of the target rate for $\gamma = 20\text{dB}$ and $\text{IRR}_t = \text{IRR}_r = 20\text{dB}$. It is obvious that the effect of RX IQI is far more significant than TX IQI only. This is because TX causes interference from the transmit signal only and not the noise or the channel gain as in RX IQI. For instance, for $R = 4\,\text{bits/s/Hz}$, TX IQI increases the OP of U_2 by more than 110%, whereas RX IQI increases it by more than 980%.

Fig. 3 illustrates the average OP of MC NOMA systems for $R = 1.25\,\text{bits/s/Hz}$. Again, we observe the significant impact of IQI on MC NOMA based systems. In fact, we notice that both TX and RX IQI cause a relatively constant shift of the average OP where the performance penalty caused by TX IQI only is fairly small and could be neglected. On the contrary, the effects of RX IQI are quite significant and require compensation in order to achieve a reliable communication link. Furthermore, it is highlighted that this impairment can alter the optimum power allocation amongst the involved users.

Finally, Fig. 4 displays the OP of a 3 user MC NOMA system vs the IRR, assuming joint TX/RX IQI with $\text{IRR}_t = \text{IRR}_r$. For the indicaive case of $R = 0.9\,\text{bits/s/Hz}$ and $\gamma = 20\text{dB}$, it is observed that, even though the level of OP increase

[1]The analysis of imperfect CSI is out of the scope of this paper and can be found in [7].

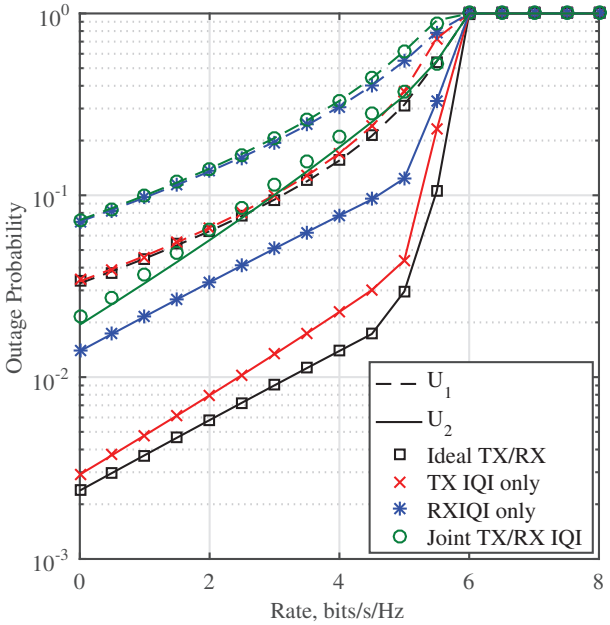

Fig. 2: OP as a function of the target rate with $\text{IRR}_t = \text{IRR}_r = 20\text{dB}$, $\gamma = 20\text{dB}$ and $\phi = 3°$.

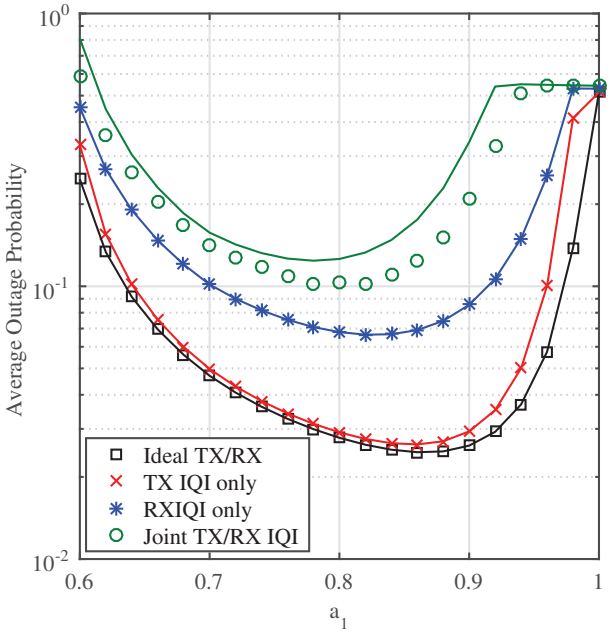

Fig. 3: Average OP as a function of a_1 for $\gamma = 20\text{dB}$, $R = 1.25\,\text{bits/s/Hz}$, $\text{IRR}_t = \text{IRR}_r = 20\text{dB}$ and $\phi = 3°$.

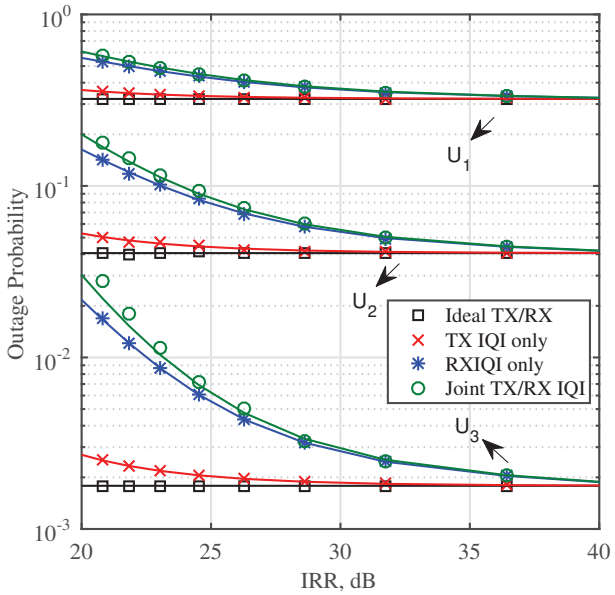

Fig. 4: OP as a function of the IRR for 3 user NOMA system with $R = 0.9\,\text{bits/s/Hz}$, $\gamma = 20\text{dB}$ and $\phi = 1°$.

depends on the user index, IQI causes a significant degradation of the OP of all NOMA users. In fact, for a relatively high IRR of 30dB, joint TX/RX IQI increases the OP of U_3 by nearly 68%, while the OP of U_1 is increased by approximately 13%.

V. Conclusion

This analysis investigated the effects of IQI on the OP of MC NOMA based systems. The realistic case of joint TX/RX IQI was considered and the corresponding OP of the considered set up was derived. Capitalizing on this, the asymptotic diversity of the considered MC NOMA system was also derived. The derived analytic results were corroborated with respective results from computer simulations. It was shown that the level of performance degradation caused by IQI depends on numerous factors, including the power allocation ratio, the impairment scenario, the target rate and the order of the considered user. This is due to the uncanceled interference from IQI that affects the performance of the employed SIC. Hence, in MC NOMA systems both the SIC and the orthogonality of the subcarriers are compromised, leading to significant performance degradation. Moreover, it was shown that IQI can deviate the optimum power splitting ratio and hence compromise the efficiency of MC NOMA systems. To this effect, this highlights the importance of effective modeling, optimization and compensation methods that will guarantee the efficient implementation of the NOMA paradigm, in the context of future communication systems, such as 5G and beyond.

Appendix A
Derivation of the OP of MC NOMA systems Impaired by Joint TX/RX IQI

It is highlighted that the j^{th} user is required to detect the messages intended for all users allocated a higher power ratio than itself before detecting its own message.

Without loss of generality, let the channel gains of all users be sorted in an ascending order as $|h_1|^2 \leq |h_2|^2 \leq ... \leq |h_M|^2$. Then, the power allocation coefficients are chosen such that $a_1 > a_2 > ... > a_M$. Assuming $1 < m < j$, the outage probability is defined as the probability that user j cannot detect its own signal or the signal intended for any user in the SIC ($j > m$), which is represented as

$$P_{(out,j)} = 1 - \Pr\left\{E^c_{j\to 1} \bigcap \cdots \bigcap E^c_{j\to j}\right\} \tag{28}$$

where

$$E_{j\to m} = \{R_{j\to m} < R_m\} \tag{29}$$

is the event that the j^{th} user cannot detect the m^{th} user's message. Also, $R_{j\to m}$ denotes the rate for the j^{th} user to detect the m^{th} user's message, R_m is the targeted data rate of the m^{th} user and $E^c_{j\to m}$ the complementary set of $E_{j\to m}$. Hence, from (28), the OP of the j^{th} sorted user is obtained as

$$P_{\text{out},j} = 1 - \Pr\{\rho_j > \psi_m\} \tag{30}$$

$$= F_{\rho_j}(\psi_m) \tag{31}$$

where $F_X(x)$ denote the CDF of X and ψ_m is given in (20). Considering the instantaneous SINR per symbol of the m^{th} user's message at the j^{th} user given in (14), for a given $\rho_j(-k)$, and making use of order statistics, it follows that the conditional SINR CDF is expressed as

$$F_{\rho_{j\to m}}(\phi_m|\rho_j(-k)) = \sum_{l=1}^{M}\left(\exp\left(-\frac{\mathcal{A}_5+\mathcal{A}_6}{\overline{\gamma}(\mathcal{A}_7-\mathcal{A}_8)}\right)\right)^{M-l} \times \binom{M}{l}\left(1-\exp\left(-\frac{\mathcal{A}_5+\mathcal{A}_6}{\overline{\gamma}(\mathcal{A}_7-\mathcal{A}_8)}\right)\right)^{l} \tag{32}$$

where $\mathcal{A}_5$, $\mathcal{A}_6$, $\mathcal{A}_7$ and $\mathcal{A}_8$ are given by

$$\mathcal{A}_5 = \phi_m\rho_j(-k)\left(|\xi_{22_j}|^2(1-a_m) + |\xi_{21_j}|^2\right), \tag{33}$$

$$\mathcal{A}_6 = \phi_m\Xi_{r_j} - |\xi_{22_j}|^2\rho_j(-k)\,a_m, \tag{34}$$

$$\mathcal{A}_7 = |\xi_{11_j}|^2 a_m \tag{35}$$

and

$$\mathcal{A}_8 = \phi_m \left(|\xi_{11_j}|^2 (1 - a_m) + |\xi_{12_j}|^2 - \sum_{i=m+1}^{M} a_i \right) \quad (36)$$

where

$$\phi_m = 2^{R_m} - 1. \quad (37)$$

It is noted that (32) is valid for the range in (23), since otherwise, the OP is unity. Based on this, the unconditional CDF is obtained by integrating (32) over the distribution of $\rho_j(-k)$, namely the Rayleigh PDF in the considered scenario. Hence, expanding the binomial and carrying out some algebraic manipulations along with evaluating the involved integral, equation (18) is deduced, which completes the proof.

REFERENCES

[1] S. M. R. Islam, N. Avazov, O. A. Dobre, and K. S. Kwak, "Power-domain non-orthogonal multiple access (NOMA) in 5G systems: Potentials and challenges," *IEEE Commun. Surveys Tuts*, vol. 19, no. 2, pp. 721–742, Secondquarter 2017.

[2] L. Dai, B. Wang, Y. Yuan, S. Han, C. l. I, and Z. Wang, "Non-orthogonal multiple access for 5G: solutions, challenges, opportunities, and future research trends," *IEEE Commun. Mag.*, vol. 53, no. 9, pp. 74–81, Sep. 2015.

[3] Y. Yuan, Z. Yuan, G. Yu, C. H. Hwang, P. K. Liao, A. Li, and K. Takeda, "Non-orthogonal transmission technology in LTE evolution," *IEEE Commun. Mag.*, vol. 54, no. 7, pp. 68–74, July 2016.

[4] S. Mirabbasi and K. Martin, "Classical and modern receiver architectures," *IEEE Commun. Mag.*, vol. 38, no. 11, pp. 132–139, Nov 2000.

[5] S. Bernard, "Digital communications fundamentals and applications," *Prentice Hall, USA*, 2001.

[6] B. Selim, S. Muhaidat, P. C. Sofotasios, A. Al-Dweik, B. S. Sharif, and T. Stouraitis, "Radio frequency front-end impairments in non-orthogonal multiple access systems," *Submitted to IEEE Veh. Technol. Mag.*, 2017. [Online]. Available: https://www.dropbox.com/s/wivpha5k1hiip58/NOMA.pdf?dl=0

[7] Z. Yang, Z. Ding, P. Fan, and G. K. Karagiannidis, "On the performance of non-orthogonal multiple access systems with partial channel information," *IEEE Trans. Commun.*, vol. 64, no. 2, pp. 654–667, Feb 2016.

[8] Z. Ding, Z. Yang, P. Fan, and H. V. Poor, "On the performance of non-orthogonal multiple access in 5G systems with randomly deployed users," *IEEE Signal Process. Lett.*, vol. 21, no. 12, pp. 1501–1505, Dec 2014.

[9] Y. Saito, Y. Kishiyama, A. Benjebbour, T. Nakamura, A. Li, and K. Higuchi, "Non-orthogonal multiple access (NOMA) for cellular future radio access," in *IEEE 77th Vehicular Technology Conference (VTC Spring)*, June 2013, pp. 1–5.

[10] T. Schenk, *RF imperfections in high-rate wireless systems: impact and digital compensation*. Springer Science & Business Media, 2008.

[11] ——, *RF Imperfections in High-Rate Wireless Systems*. The Netherlands: Springer, 2008.

[12] S. J. Grant and J. K. Cavers, "Analytical calculation of outage probability for a general cellular mobile radio system," in *Gateway to 21st Century Communications Village. VTC 1999-Fall. IEEE VTS 50th Vehicular Technology Conference (Cat. No.99CH36324)*, vol. 3, 1999, pp. 1372–1376 vol.3.

[13] M. Uysal, "Diversity analysis of space-time coding in cascaded Rayleigh fading channels," *IEEE Commun. Lett.*, vol. 10, no. 3, pp. 165–167, Mar 2006.